

Anisotropy of the Debye-Waller factor in cesium-graphite intercalation compounds by Mössbauer spectroscopy, and the quadrupole moment of the 81-keV state in $^{133}\text{Cs}^\dagger$

L. E. Campbell,* G. L. Montet, and G. J. Perlow

Argonne National Laboratory, Argonne, Illinois 60439

(Received 1 October 1976)

Mössbauer-effect measurements are reported in the lamellar compounds C_8Cs and C_{24}Cs . The experiments utilized the 81-keV transition from the $5/2^+$ first excited to the $7/2^+$ ground state in ^{133}Cs . The C_8Cs samples were made from ordered pyrolytic graphite and exhibited a highly anisotropic recoilless fraction which at 4.2 K was approximately 20 times greater along the c axis than perpendicular to it. The magnitude and sign of the quadrupole coupling of the $5/2^+$ excited state was measured [$+4.29(5) \times 10^{-7}$ eV] and combined with an NMR value for the ground-state coupling to give $|Q_{\text{ex}}/Q_{\text{gr}}| = 88 \pm 6$. The sign of eq was determined to be negative on the basis of simple models of the cesiated-graphite lattice, resulting in the value $Q_{\text{ex}} = -0.22(5)$ b. The negative sign and the magnitude are in accord with the trend of low-lying $5/2^+$ states in this region of neutron number. Isomer-shift values indicate that the Cs is fully ionized in C_{24}Cs and approximately 50% ionized in C_8Cs .

I. INTRODUCTION

We report here Mössbauer-effect measurements on graphite intercalation compounds of Cs.^{1,2} Recoilless γ -ray absorption of the 81-keV γ ray from ^{133}Cs was used to study (i) the anisotropy of the Debye-Waller factor, (ii) the quadrupole moment of the first-excited nuclear state in ^{133}Cs , and (iii) the ionic state of Cs in these compounds. The samples studied were used as absorbers in transmission geometry. All measurements were made at 4.2 K.

The recoilless fraction for the Mössbauer effect is given by the Debye-Waller factor and under fairly general conditions of binding can be written

$$f = e^{-\langle (\vec{k} \cdot \vec{r})^2 \rangle}, \quad (1)$$

where \vec{k} is the wave vector of the γ ray, \vec{r} is the displacement of the nucleus from its equilibrium position, and $\langle \rangle$ indicates an average over the thermal motion of the nucleus. If the forces which bind the atom in the crystal are anisotropic, the argument of the exponential will depend on the direction of \vec{k} with respect to the crystalline axes of the sample, and the recoilless fraction observed in a single-crystal absorber will depend on the orientation of the absorber with respect to the γ -ray beam. We have measured the variation of f with direction in the pyrolytic graphite intercalation compound C_8Cs . Pyrolytic graphite¹ consists of small graphite crystals all of whose c axes are fairly well aligned but whose a and b axes are randomly oriented with respect to each other in the plane perpendicular to c . As there is local sixfold symmetry for rotations about the c axis,

the pyrolytic graphite for the purposes of our experiments acts like an aligned but imperfect single crystal. We observed approximately a factor of 20 variation in f between observations parallel and perpendicular to the c axis.

The ground nuclear state of ^{133}Cs has $I^\pi = \frac{7}{2}^+$ but an extremely small quadrupole moment. The quadrupole moments for the ground state of odd-mass nuclei just heavier are positive, and for those just lighter are negative, cesium being at the point of the sign change. It is therefore of interest to determine the magnitude and sign of the quadrupole moment of the $\frac{5}{2}^+$ low-lying first-excited state, Q_{ex} . The extreme anisotropy of the graphite lattice provides a sufficiently large electric field gradient (EFG) defined by $eq \equiv \partial^2 V / \partial z^2$, to produce a measurable splitting of this state. Since the absorber is highly ordered, the relative intensities of the absorption lines give the sign of the quadrupole coupling $e^2 q Q_{\text{ex}}$ (it is positive). An NMR measurement of the splitting of the ground state in the same compound allows us to determine the ratio of the excited-state to ground-state moment. We get $|Q_{\text{ex}}/Q_{\text{gr}}| = 88 \pm 6$. From this and the somewhat uncertain value of Q_{gr} we have obtained $|Q_{\text{ex}}| = 0.22(5)$ b. We discuss the disposition of charges in the lattice and conclude that the EFG is in all likelihood negative. And therefore with the same likelihood the quadrupole moment Q_{ex} is also negative.

Optical³ and NMR⁴ measurements on C_8Cs suggest that the cesium in this lattice is not completely ionized while similar measurements on C_{24}Cs indicate complete ionization. Our isomer-shift values confirm those conclusions, and give a Cs atomic configuration of $6s^{0.5}40.2$.

II. GRAPHITE-Cs INTERCALATION COMPOUNDS

Graphite usually crystallizes in a layer lattice in which the carbon atoms form regular sheets of linked hexagons which are displaced relative to one another. In the stable hexagonal modification, alternate sheets are laterally displaced from each other so that the stacking sequence is $\cdots ABAB \cdots$, and the identity period along the c axis is twice the layer plane separation. Within the layer planes each carbon atom is strongly bonded to its neighbors while the bonding between layers is substantially weaker. Consequently a suitable reactant is often able under quite mild conditions to become intercalated between the carbon planes. When this occurs the carbon planes remain intact but their separation increases.

The alkali metals potassium, rubidium, and cesium react readily with graphite to form intercalation compounds whose chemical and physical properties are similar. Compounds which have been reported are C_8M , $C_{10}M$ (stable only above about 300°C), $C_{24}M$, $C_{36}M$, $C_{48}M$, and $C_{60}M$ where M represents either potassium, rubidium, or cesium.

The crystal structure of these compounds has been established by Rudorff and Schulze⁵ by x-ray diffraction. Figure 1 shows the positions of the Cs atoms relative to the carbon hexagons. In $C_8\text{Cs}$ the carbon and cesium layers alternate, with each carbon lattice differing from the others by a simple translation along the c axis. The cesium layers, however, are displaced in the basal plane relative to each other and so the complete stacking sequence is $\cdots AaAbAcAdAa \cdots$, where lower-case letters refer to Cs configurations. In $C_{24}\text{Cs}$ there are two carbon layers for each Cs layer and the stacking sequence is $\cdots A \text{ Cs } AB \text{ Cs } BA \cdots$. In order to accommodate the cesium atoms, the distance between the graphite layers in all the various

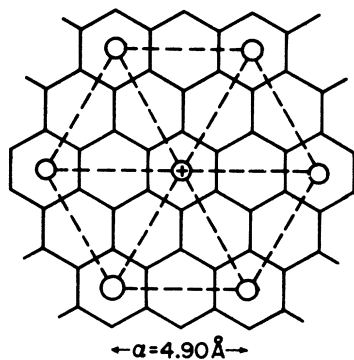


FIG. 1. Positions of the Cs atoms relative to the carbon lattice. Central Cs atom marked \oplus is not present in $C_{24}\text{Cs}$.

stages increases from the original 3.35 to 5.95 \AA . In both $C_8\text{Cs}$ and $C_{24}\text{Cs}$ the Cs-Cs distance is 4.90 \AA in the plane. The C-C bond distance is 1.415 \AA .

This description of graphite and its alkali-metal intercalation compounds refers to the ideal structures. The pyrolytic graphite used in these studies is not ideal although in its annealed form it approaches ideality. It can be characterized by the angular dispersion of the c axes of the individual crystallite domains ($\theta_{1/2} \sim 7$ and 15° for our annealed and unannealed samples, respectively), and the mean crystallite dimensions L_c and L_a along the c and a axes. The latter were $\sim 1000 \text{ \AA}$ for an annealed sample.

III. DESCRIPTION OF SAMPLES AND MEASUREMENTS

Three different disk shaped absorbers were used. (i) A $C_8\text{Cs}$ absorber made from annealed pyrolytic graphite containing $0.138 \text{ (g Cs)/cm}^2$ whose c axis was perpendicular to the plane of the sample. This was used in measurements at angles ranging from 0 to 30° . (ii) A $C_8\text{Cs}$ absorber made from unannealed pyrolytic graphite containing $0.286 \text{ (g Cs)/cm}^2$, whose c axis was parallel to the plane of the sample. It was used in measurements at angles ranging from 45 to 90° . (iii) A $C_{24}\text{Cs}$ absorber made from polycrystalline graphite and containing $0.294 \text{ (g Cs)/cm}^2$.

All samples were prepared by the two-bulb technique¹ in which triply distilled cesium was maintained at 250°C , and high-purity graphite at 350°C . The reaction was usually allowed to proceed overnight. The pyrolytic graphite had been initially deposited at a high temperature ($\sim 2500^\circ\text{C}$) and annealed for $\frac{1}{2}$ hat 3250°C . All operations were carried out in vacuum and the cesium-graphite compound was sealed into a thin Pyrex cell. To ensure thermal contact with the liquid-helium bath, a low pressure of He gas was then diffused into the cell. Two independent methods were used to determine the amount of cesium in the samples. (a) The graphite disks were measured and weighed before the preparation of each sample and the amount of intercalated cesium was calculated assuming the stoichiometric amounts of cesium and carbon. (b) A γ -ray absorption measurement utilizing the 122 keV radiation from ^{57}Fe was made on sample 1. A Ge(Li) detector was used to measure the atomic absorption of graphite samples with and without the intercalated cesium present. The results obtained by these two methods agreed within 1% .

The velocity spectrometer used in this work is the same one used in several earlier investigations.⁶ It is a mechanical sinusoidal drive in which

both source and absorber are immersed in liquid helium. The source was a ^{133}Ba aluminum alloy of nominal composition BaAl_4 . ^{133}Ba decays by electron capture to ^{133}Cs . The transition from the first-excited state of ^{133}Cs ($\frac{5}{2}^+$) to the ground state ($\frac{7}{2}^+$) is 97.4% $M1$ + 2.6% $E2$,⁷ and gives rise to the 81 keV Mössbauer γ ray. Decays from the second- to the first-excited state produced an 80 keV γ -ray which could not be resolved from the 81-keV line. It constitutes 7% of the total line seen by the counter. The recoilless fraction f_s of the source had been measured previously⁸ and found to be $(6.6 \pm 0.6) \times 10^{-2}$. The size of the source and a collimator at the counter served to collimate the γ -ray beam to $\pm 6^\circ$. The Doppler shifting was done by moving the absorber. The γ rays were detected in a Ge(Li) detector with a resolution of about 3 keV. Good energy resolution is necessary in order to decrease the magnitude of the background correction needed in the f -factor calculation. The background was typically 20% of the total.

IV. DATA ANALYSIS

Equation (2) is the quadrupole interaction Hamiltonian which is to be applied to both the ground- and excited-state manifolds. Figure 2 is the resulting energy-level diagram for the $\frac{5}{2}^+ - \frac{7}{2}^+$ case.

$$\mathcal{H} = \frac{e^2 q Q}{4I(2I-1)} [3I_z^2 - I(I+1) + \frac{1}{2}\eta(I_+^2 + I_-^2)]. \quad (2)$$

In the diagram η has been assumed equal to zero because the local environment of the Cs ion has sixfold symmetry about the c axis and the a and b axes of the individual crystallites are randomly oriented in the basal plane. The splitting of the ground state has been neglected at this point since it is small compared to the natural linewidth (1.4%). The diagram is drawn for positive quadrupole coupling in the excited state. The theoretical relative absorption cross sections for each of the three lines have been calculated⁹ as a function of angle θ and mixing parameter $\delta = -0.16$ and are given by the following expressions.

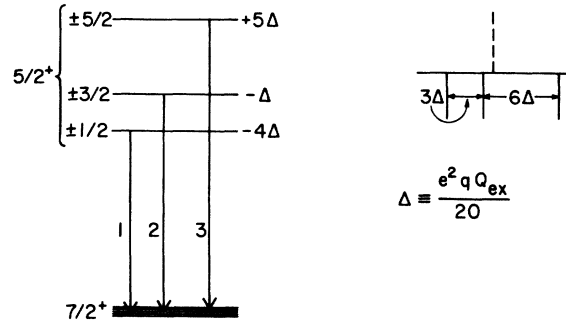


FIG. 2. Quadrupole splitting of the ^{133}Cs first-excited state and corresponding emission spectrum.

$$\begin{aligned} F_1(\theta) &= (0.911 + 0.744\delta^2) \\ &\quad + (0.268 + 0.928\delta + 0.685\delta^2) \cos^2\theta \\ &\quad + 0.928\delta \cos 2\theta + 0.060\delta^2 \cos^2 2\theta, \\ F_2(\theta) &= (1.018 + 1.161\delta^2) \\ &\quad - (0.054 + 0.189\delta + 0.232\delta^2) \cos^2\theta \\ &\quad - 0.186\delta \cos 2\theta - 0.179\delta^2 \cos^2 2\theta, \\ F_3(\theta) &= (1.072 + 1.095\delta^2) \\ &\quad - (0.214 + 0.742\delta + 0.452\delta^2) \cos^2\theta \\ &\quad - 0.742\delta \cos 2\theta + 0.119\delta^2 \cos^2 2\theta. \end{aligned} \quad (3)$$

The cross sections have been evaluated at the angles used in the experiment and are displayed in Table I. A typical Mössbauer spectrum is shown in Fig. 3, and inspection of this figure in the light of Fig. 2 and Table I indicates clearly that the sign of the quadrupole coupling is positive.

Since the three absorption lines overlap considerably, fitting the data with sums of Lorentzian curves will result in inaccurate values for the line positions and the recoil-free fractions.¹⁰ For this reason we used a fitting procedure that evaluated the transmission integral shown in Eq. (4).

$$N(\epsilon) = (1 - f_s) + \frac{1}{S_0} \int_{-\infty}^{\infty} dE S(E - \epsilon) e^{-\sigma(E) f_a n_a}. \quad (4)$$

TABLE I. Relative resonant cross sections $F_i(\theta)$ at angles of interest for the $M_1 + E_2$ transitions of Fig. 1. Calculation based on $\delta = -0.16$. The values are normalized to $\sum_i F_i(\theta) = 3$.

θ (deg)	0	15	30	45	60	75	90
F_1	0.897	0.907	0.935	0.973	1.013	1.042	1.053
F_2	1.017	1.016	1.013	1.007	0.999	0.991	0.988
F_3	1.086	1.077	1.052	1.020	0.988	0.967	0.959

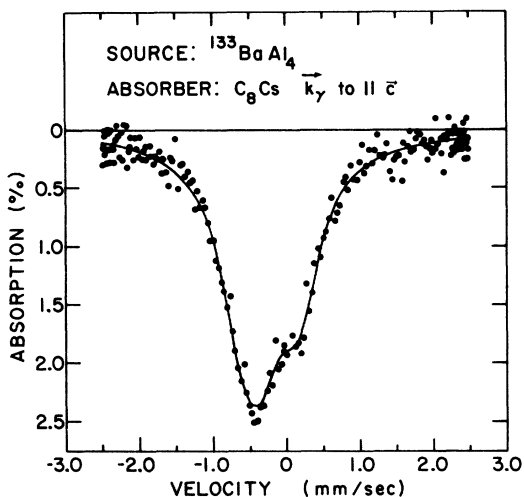


FIG. 3. Typical velocity spectrum for C_8Cs at 4.2 K. γ -ray beam is parallel to the c axis (i.e., $\theta=0$). Source is $^{133}BaAl_4$.

Here $N(\epsilon)$ is the normalized counting rate as a function of the Doppler energy shift ϵ , $S(E)$ describes the energy distribution of the recoilless radiation from the source, and $\int_0^\infty S(E)dE = f_s S_0$. It was assumed that $S(E)$ was a Lorentzian having a width of 0.357 mm/sec deduced from earlier work with this source. $\sigma(E)f_a n_a$ was represented by the sum of three Lorentzian lines whose widths were set equal to the natural width of the absorption line (0.267 mm/sec), and whose positions and heights were searched on by the computer during the fitting process. In such fittings, the positions were generally constrained to be consistent with the assumption that $\eta = 0$ and the heights were always constrained to have the ratios predicted by theory (Table I). The transmission integral was evaluated by Gaussian integration.¹¹

With the aid of this program e^2qQ_{ex} , the isomer shifts and their standard errors were obtained for

each of twelve different C_8Cs spectra. Weighted average values for both quantities were obtained using the $1/\sigma^2$ as the weighting factors. Isomer shift and quadrupole splitting values were also obtained from a $C_{24}Cs$ spectrum. These values are displayed in Table II. As a matter of interest we also give values for the same quantities obtained from standard Lorentzian fitting procedures. The two differ, as expected. Since the transmission integral program also searched on the intensities, values of the recoils fraction could be calculated directly from f_s and the fitting parameters t_i :

$$t_i = n(\theta)f_a(\theta)\sigma_0 F_i(\theta)/3. \quad (5)$$

Here the subscript i labels each of the three lines in turn, f_s and f_a refer to source and absorber, respectively, σ_0 is the Breit-Wigner cross-section at resonance [$1.017(17) \times 10^{-19} \text{ cm}^2$], $n(\theta)$ is the sample thickness in atoms of Cs per cm^2 , and the $F_i(\theta)$ are the tabulated relative angular factors of Table I. The factor $\frac{1}{3}$ arises from their normalization. Measured values of f_a as a function of the angle θ between the absorber c axis and the γ -ray beam are given in Table III and plotted in Fig. 4.

The transmission integral disregards the polarization-dependent saturation discussed by Housley *et al.*¹² which can be important for thick highly ordered absorbers such as ours. However, the near degeneracy of the nuclear ground-state manifold leads to very small polarizations. A calculation showed the effect to be undetectable in our experiments.

V. RESULTS AND DISCUSSION

A. Recoilless fraction in C_8Cs

Equation (1) is a general expression for the recoilless fraction f . In a single crystal with at least threefold symmetry about the c axis one may characterize the nuclear motion with just two parameters: $\langle x^2 \rangle = \langle y^2 \rangle$, and $\langle z^2 \rangle$, where here the

TABLE II. Average values of quadrupole coupling and isomer shift of the first-excited state of ^{133}Cs in C_8Cs and $C_{24}Cs$.

	C_8Cs		$C_{24}Cs$
	Transmission integral fit	Simple Lorentzian fit	Transmission integral fit
e^2qQ_{ex} (mm/sec)	1.59 ± 0.02	1.68 ± 0.01	1.54 ± 0.08
(eV)	$4.29(5) \times 10^{-7}$	$4.54(3) \times 10^{-7}$	
Isomer shift (mm/sec)	-0.249 ± 0.003	-0.235 ± 0.003	-0.303 ± 0.016
Derived quantities:	$ Q_{ex}/Q_{gr} = 88 \pm 6$		
	$Q_{ex} = -0.22(5) \text{ b}$		

TABLE III. Angular variation of recoil-free fraction f_a , corresponding mean-square Cs atomic displacement $\langle(\vec{r} \cdot \hat{k})^2\rangle$ along the observation direction, best-fit Debye-Waller parameters from Eq. (6), and corresponding characteristic temperatures Θ_{\parallel} and Θ_{\perp} .

θ (deg)	0	0	15	30	45	60	75	90
f_a : measured (%)	3.77(7)	4.26(8)	3.38(7)	2.28(5)	1.19(4)	0.57(3)	0.26(2)	0.18(1)
f_a : fit to Eq. (6) (%)	4.15	4.15	3.42	2.03	0.99	0.48	0.29	0.24
$\langle(\vec{r} \cdot \hat{k})^2\rangle$: measured (10^{-4} \AA^2)	19.5	18.7	20.1	22.4	26.3	30.6	35.2	37.5
$\langle(\vec{r} \cdot \hat{k})^2\rangle$: fit (10^{-4} \AA^2)	18.9	18.9	20.0	23.1	27.4	31.7	34.7	35.8
Best-fit parameters:	$\langle x^2 \rangle = 35.8(3) \times 10^{-4} \text{ \AA}^2$			$\Theta_{\parallel} = 76.5 \text{ K}$				
	$\langle z^2 \rangle = 18.9(1) \times 10^{-4} \text{ \AA}^2$			$\Theta_{\perp} = 145 \text{ K}$				

z axis coincides with the c axis. This is the situation in C_8Cs . If \vec{k} makes an angle θ with the c axis, one may write for the Debye-Waller factor¹³:

$$f(\theta) = \exp[-k^2(\langle z^2 \rangle - \langle x^2 \rangle) \cos^2 \theta - k^2 \langle x^2 \rangle]. \quad (6)$$

The experimental results are displayed in Fig. 4 and Table III. Included in Fig. 4 is a least-squares fit of the function in Eq. (6) to the experimental points. Table III includes the values of the parameters $\langle x^2 \rangle$ and $\langle z^2 \rangle$ which gave the best fit, along with the corresponding characteristic temperatures. Inspection of Fig. 4 and Table III shows the remarkable angular variation of the recoil-free fraction. It decreases by a factor of 20 between 0 and 90°. The variation in the exponent of the Debye-Waller factor is of course much less.

The quoted errors and error bars on $f_a(\theta)$ are those obtained by fitting the spectra. In addition there are errors associated with f_s , with absorber thickness, and with background subtraction. The latter is presumably responsible for the discrepancy in the two values of $f_a(0)$. The values for $f(75^\circ)$ and $f(90^\circ)$ may be as much as 10% low owing to fractures in the sample. Besides these there are errors caused by the finite collimation (6.6°) and by the angular spread of the crystalline c axes. A straightforward calculation shows that in the worst case the effect of the collimation upon f_a is to introduce an error of 0.75%, and that the angular dispersion of c axes has a comparably small effect. Both can safely be ignored. To obtain the fit to Eq. (6) we have roughly but adequately taken all extra sources of error into account by doubling the quoted statistical error for each point. The errors we quote for $\langle x^2 \rangle$ and $\langle z^2 \rangle$ are then obtained from the variation of χ^2 in the neighborhood of its minimum in the fitting process.

It is interesting to compare the values of $\langle x^2 \rangle$ and $\langle z^2 \rangle$ determined here at 4.2 K for Cs in graphite with the corresponding values for the carbon atoms in pure graphite. The graphite values are well known.^{14,15} The mean-square displacements are quoted in terms of characteristic temperatures

Θ_{\perp} and Θ_{\parallel} , where, for example,

$$\langle z^2 \rangle = (3\hbar^2/Mk_B\Theta_{\perp})[(T/\Theta_{\perp})\Phi(\Theta_{\perp}/T) + \frac{1}{4}]. \quad (7)$$

The appropriate values for carbon are $\Theta_{\perp} = 800 \text{ K}$ and $\Theta_{\parallel} = 2400 \text{ K}$ corresponding to $\langle x^2 \rangle_c = 12.5 \times 10^{-4} \text{ \AA}^2$ and $\langle z^2 \rangle_c = 37.6 \times 10^{-4} \text{ \AA}^2$, at $T = 0$. Displacements within the basal plane are much smaller than those out of the plane because of the strong binding between carbon atoms within each plane. Exactly the *opposite* is true for the Cs in C_8Cs . Here the atom of interest is more tightly constrained in the c (i.e., z) direction by the carbon planes but relatively more free to move back and forth between the planes. In fact, $\langle z^2 \rangle$ for cesium in C_8Cs is considerably less than that for carbon in the pure graphite lattice, $18.9 \times 10^{-4} \text{ \AA}^2$ compared to $37.6 \times 10^{-4} \text{ \AA}^2$. On the other hand, $\langle x^2 \rangle$ for Cs in C_8Cs is much greater than that for the carbon atoms, $35.8 \times 10^{-4} \text{ \AA}^2$ compared to $12.5 \times 10^{-4} \text{ \AA}^2$.

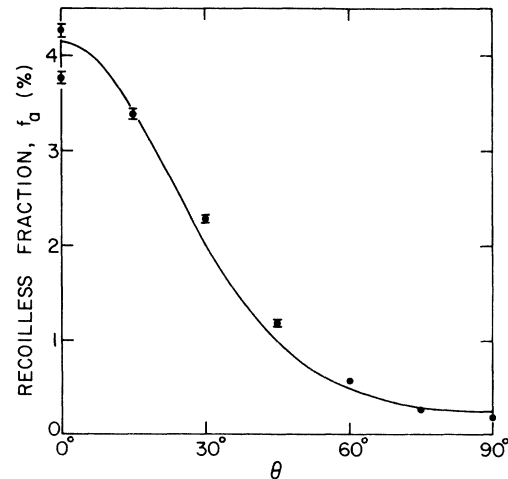


FIG. 4. Recoilless fraction values f_a as a function of θ . Smooth curve is a least-squares fit of Eq. (6) to the data.

B. Quadrupole moment of ^{133}Cs (81-keV state) and the EFG in C_8Cs and C_{24}Cs

Carver⁴ has measured the ground-state quadrupole interaction energy in C_8Cs by NMR and finds the average spacing between the individual quadrupole split lines to be 75 ± 5 G. From this one gets a value¹⁶ of 84 ± 6 kHz for $\nu_Q = e^2qQ/14h$ and $(4.88 \pm 0.33) \times 10^{-9}$ eV for $|e^2qQ|$. Using this result and our measurements for C_8Cs (see Table II) we are able to arrive at a value for the ratio of the excited- and ground-state quadrupole moments $|Q_{\text{ex}}/Q_{\text{gr}}| = 88 \pm 6$. The ground-state quadrupole moment Q_{gr} has been measured and this allows us to obtain a value for $|Q_{\text{ex}}|$. Since Q_{gr} is so small, more than the usual uncertainties are associated with its value. Rydberg¹⁷ quotes $Q_{\text{gr}} = -0.003(1)$ b by level crossing spectroscopy including internal Sternheimer correction.¹⁸ O'Reilly and Peterson¹⁹ compared NMR relaxation rates of $^{133}\text{Cs}^+$ and $^{87}\text{Rb}^+$ in aqueous solution. The ratio leads to the ratio of the two quadrupole moments after application of the external Sternheimer correction $1 - \gamma_\infty$ appropriate for each ion. They quote $0.0023(3)$ b for ^{133}Cs . With the present values^{20,21} of γ_∞ and Q of ^{87}Rb , this becomes $|Q_{\text{gr}}| = 0.0021$ b. The relaxation method contains uncertainties not included in the error estimate. In the absence of better knowledge we may take the simple average of the two measurements, $Q_{\text{gr}} = -0.0025(5)$ b for the ground-state moment. With this we obtain for the magnitude of the quadrupole moment of the 81-keV ($\frac{5}{2}^+$) first-excited state of ^{133}Cs , $|Q_{\text{ex}}| = 0.22 \pm 0.05$ b.

Our analysis has given us the magnitude and sign of e^2qQ_{ex} ($+4.29(5) \times 10^{-7}$ eV), the magnitude of Q_{ex} , and hence the magnitude of eq . A determination of the sign of eq would give the sign of Q_{ex} . We have performed a variety of C_8Cs lattice sums for this purpose. Results are given in Table IV for the quantity eq_{lattice} . The relation of eq_{lattice} to eq is given by the external Sternheimer factor, eq (at the nucleus) = $(1 - \gamma_\infty) \times eq_{\text{lattice}}$. The sum over the Cs^+ ions gives a negative contribution of the right order of magnitude, but it must be reduced by about 50% to account for the incomplete ionization. The Cs electron contribution is to be reduced by the same factor. Here the electrons are assumed to be uniformly distributed throughout the volume following the procedure of deWette.²² In the case of noncubic metals, for example, it is well known that such an assumption is unwarranted.²³ The corresponding sums are also carried out for the carbon atoms assumed to have given up y electrons per atom to conduction bands. For graphite alone, y is sufficiently small ($\sim 10^{-4}$) to give a negligible contribution. A calculation assuming the source of the EFG to be quadrupoles

TABLE IV. Calculated value for eq_{lattice} by lattice summation. Entries are in units of 10^{13} esu/cm³.

	eq_{lattice}
Cs^{1+}	-4.5
Cs conduction electrons (uniform distribution)	+3.3
C^{3+}	-0.31y
C conduction electrons [(y electrons)/(C atom) uniformly distributed]	+26y
"Carbon p_x quadrupole"	+0.20
Conducting sheet model with $\text{Cs}^{0.5+}$	-2.2
Experimental value	± 6.3

derived from p_x orbitals on the carbon atoms gives a negligible contribution also.

There is evidence that the electrons from the Cs are concentrated in the carbon planes.²⁴ The lattice sum with 0.5 electron on each Cs and 0.5/8 on each carbon leads to $eq_{\text{lattice}} = -2.23$. This is unrealistic however, because C_8Cs is metallic. The electron density can shift to screen the electric fields. As a model we can consider a two-dimensional net of Cs ions of charge +0.5 confined within conducting plates at the mean separation of the carbon planes. We assume that fields external to the planes are screened out. It is clear that the screening cannot be complete however, as there are not electrons available with wave numbers shorter than the Fermi wave number k_F . It has been shown that this leads to an oscillatory behavior of the EFG with distance.²³ In this model this would apply to contributions from outside the conducting planes and is likely to be small. Within, the EFG may be evaluated by the method of images. We have performed such a sum approximately and obtain $eq_{\text{lattice}} = -2.2 \times 10^{13}$ esu/cm³. Although the model is very simple, inspection of the partial sums leads us to the belief that improvements cannot alter the negative sign of the EFG. With this, the sign of the nuclear excited-state quadrupole moment is also negative, and we get $Q_{\text{ex}} = -0.22(5)$ b. The negative value for Q_{ex} is in general accord with the sign and the trend of the magnitudes of the quadrupole moments of the ground or low-lying $\frac{5}{2}^+$ states in the region just below the closed $N = 82$ neutron shell.^{25,26}

C. Ionization state in C_8Cs

Optical transmission experiments by Hennig³ implied that the Cs in C_8Cs is only two-thirds ionized, whereas the cesium in C_{24}Cs is completely ionized. More recently, Knight-shift measurements by Carver⁴ have confirmed this view and an

ionization of 55% was deduced for C_8Cs . A comparison of the isomer-shift data of Table II with the calibration of isomer shifts in Cs compounds by Boyle and Perlow²⁷ indicates that the ionization of Cs in C_8Cs is 0.5 ± 0.2 in agreement with results by the other methods.

ACKNOWLEDGMENTS

The authors wish to acknowledge early and stimulating discussions with the late G. R. Hennig. We have profited by discussions at various times with A. J. F. Boyle, R. D. Lawson, and D. Kurath.

*Present address: Hobart and William Smith Colleges, Geneva, N.Y. 14456.

†Work performed under the auspices of ERDA.

¹*Graphite and Its Crystal Compounds*, edited by A. R. Ubbelohde and F. A. Lewis (Clarendon, Oxford, 1960).

²G. R. Hennig, *Prog. Inorg. Chem.* **1**, 125 (1959).

³G. R. Hennig, *J. Chem. Phys.* **43**, 1201 (1965).

⁴G. P. Carver, *Phys. Rev. B* **2**, 2284 (1970); also Report No. 1283, Materials Science Center, Cornell University (unpublished).

⁵W. Rudorff and E. Schulze, *Z. Anorg. Allg. Chem.* **277**, 156 (1954).

⁶G. J. Perlow, *Mössbauer Effect Methodology* (Plenum, New York, 1967), Vol. 3, pp. 191–201.

⁷K. Siegbahn *et al.*, *Nucl. Instrum. Methods* **27**, 173 (1964).

⁸A. J. F. Boyle and G. J. Perlow, *Phys. Rev.* **151**, 211 (1966).

⁹M. E. Rose, *Multipole Fields* (Wiley, New York, 1955).

¹⁰E. Gerdau, W. Râth, and H. Winkler, *Z. Phys.* **257**, 29 (1972).

¹¹We wish to thank B. Dunlap and G. Czjzek for introducing us to this technique.

¹²R. M. Housley, U. Gonser, and R. W. Grant, *Phys. Rev. Lett.* **20**, 1279 (1968); also R. M. Housley, *Mössbauer Effect Methodology* (Plenum, New York, 1970), Vol. 5, p. 109.

¹³Yu. Kagan, *Dokl. Akad. Nauk. SSSR* **140**, 794 (1961).

¹⁴G. Albinet, J. P. Biberian, and M. Bienfait, *Phys. Rev. B* **3**, 2015 (1971).

¹⁵J. P. Biberian, M. Bienfait, and J. B. Theeten, *Acta Crystallogr. A* **29**, 221 (1973).

¹⁶The value quoted for ν_Q in Carver's paper is inconsistent with the data shown in his Fig. 5 and is incorrect. G. P. Carver (private communication).

¹⁷S. Rydberg and S. Svanberg, *Phys. Scr.* **5**, 209 (1972).

¹⁸R. M. Sternheimer and R. F. Peierls, *Phys. Rev. A* **3**, 837 (1971).

¹⁹D. E. O'Reilly and E. M. Peterson, *J. Chem. Phys.* **51**, 4906 (1969).

²⁰R. M. Sternheimer, *Phys. Rev.* **146**, 140 (1966).

²¹H. A. Schüssler, *Z. Phys.* **182**, 289 (1965).

²²F. W. deWette, *Phys. Rev.* **123**, 103 (1961).

²³See, e.g., K. Nishiyama, F. Dimmling, Th. Kornrumpf, and D. Riegel, *Phys. Rev. Lett.* **37**, 357 (1976).

²⁴F. J. Salzano and S. J. Aronson, *J. Chem. Phys.* **44**, 4320 (1966); **45**, 2221 (1966).

²⁵F. Ackermann, E. W. Otten, G. zu Putlitz, A. Schenck, and S. Ullrich, *Nucl. Phys. A* **248**, 157 (1975).

²⁶G. J. Perlow and S. L. Ruby, *Phys. Lett.* **13**, 198 (1964).

²⁷A. J. F. Boyle and G. J. Perlow, *Phys. Rev.* **149**, 165 (1966).